Title

Impaired Collateral Flow Compensation During Chronic Cerebral Hypoperfusion in the Type 2 Diabetic Mice

Journal

Stroke, 47(12)

ISSN

0039-2499

Authors

Nishijima, Yasuo
Akamatsu, Yosuke
Yang, Shih Yen
et al.

Publication Date

2016-12-01

DOI

10.1161/strokeaha.116.014882

Peer reviewed

Published in final edited form as:

Stroke. 2016 December ; 47(12): 3014–3021. doi:10.1161/STROKEAHA.116.014882.

Impaired collateral flow compensation during chronic cerebral hypoperfusion in the type-II-diabetic mice

Yasuo Nishijima, MD, PhD[1,2,3,¶], **Yosuke Akamatsu, MD, PhD**[1,2,3,¶], **Shih Yen Yang, BS**[1,2], **Chih Cheng Lee, BS**[1,2], **Utku Baran, PhD**[4], **Shaozhen Song, PhD**[4], **Ruikang K. Wang, PhD**[4], **Teiji Tominaga, MD**[3], and **Jialing Liu, PhD**[1,2]

[1]Department of Neurological Surgery, UCSF, San Francisco, CA 94121, USA

[2]SFVAMC, San Francisco, CA 94121, USA

[3]Department of Neurosurgery, Tohoku University Graduate School of Medicine, 1-1 Seiryo-machi, Aoba-ku, Sendai 980-8574, Japan

[4]Departments of Bioengineering & Ophthalmology, University of Washington, Seattle, WA 98195, USA

Abstract

BACKGROUND AND PURPOSE—The presence of collaterals is associated with a reduced risk of stroke and transient ischemic attack (TIA) in patients with steno-occlusive carotid artery disease. Although metabolic syndrome negatively impacts collateral status, it is unclear whether and to what extent type 2 diabetes (T2DM) affects cerebral collateral flow regulation during hypoperfusion.

METHODS—We examined the spatial and temporal changes of the leptomeningeal collateral flow and the flow dynamics of the penetrating arterioles in the distal MCA and ACA branches over two weeks following unilateral common carotid artery occlusion (CCAO) using optical coherent tomography in *db/+* and *db/db* mice. We also assessed the temporal adaptation of the circle of Willis (CW) following CCAO by measuring CW vessel diameters.

RESULTS—Following unilateral CCAO, *db/db* mice exhibited diminished leptomeningeal collateral flow compensation compared to *db*/+ mice, which coincided with a reduced dilation of distal ACA branches, leading to reduced flow not only in pial vessels, but also in penetrating arterioles bordering the distal MCA and ACA. However, no apparent cell death was detected in either strain of mice during the first week after CCAO. *db/db* mice also experienced a more severe early reduction in the vessel diameters of several ipsilateral main feeding arteries in the CW, in addition to a delayed post-CCAO adaptive response by one to two weeks compared to *db/+* mice.

CONCLUSIONS—T2DM is an additional risk factor for hemodynamic compromise during cerebral hypoperfusion, which may increase the severity and the risk of stroke or TIA.

Corresponding author: Dr. Jialing Liu, Department of Neurological Surgery (112C), University of California at San Francisco and Department of Veterans Affairs Medical Center, 1700 Owens Street, San Francisco, California 94158, USA. Phone: (415) 575-0407; Fax: (415) 575-0595; jialing.liu@ucsf.edu.

¶These authors contributed equally to this work.

Disclosure: None

Keywords

arteriogenesis; doppler OCT; CCAO; carotid occlusive disease; anastomosis; vascular remodeling

Introduction

The extent of cerebral collateralization directly contributes to the cerebrovascular reserve capacity, which in turn, affects the hemodynamics[1]. By the same token, cerebral collateral circulation has long been reported to alter the risk of stroke[2, 3]. In particular, among patients with chronic occlusion of the internal carotid artery or arteries, failure of collateralization may contribute to hemodynamic compromise and increased risk of stroke or transient ischemic attacks (TIA)[4, 5]. In addition, an absence of collateral circulation in the middle cerebral artery (MCA) is associated with a poor prognosis in symptomatic unilateral carotid occlusion[6]. Furthermore, patients with metabolic syndromes are associated with poor anatomical collateral status during acute ischemic stroke[7]. While corroborating experimental evidence suggests that Type II diabetes (T2DM) is associated with impaired leptomeningeal collateral compensation during MCA stroke[8, 9], it remains to be determined whether and to what extent an impaired cerebral collateral flow regulation occurs during carotid occlusion in subjects with T2DM.

The degree of cortical hypoperfusion in the forebrain following unilateral carotid steno-occlusion depends on the dynamic compensation from the contralateral carotid flow and the leptomeningeal collateral circulation as well as the posterior circulation and extracranial carotid anastomosis. As the connecting point in the collateral vessels, the anastomosis allows blood to shift between two opposing flow directions, equalizing blood volume and perfusion pressure. In the current study, we examined the spatial and temporal changes of the leptomeningeal collateral flow as well as the flow dynamics of penetrating arterioles in the distal MCA and anterior cerebral artery (ACA) following unilateral common carotid artery occlusion (CCAO) using optical coherent tomography based microangiography, and temporal changes in the diameters of the vessels forming the circle of Willis (CW) in normal and diabetic mice. Our results indicate that upon unilateral CCAO, diabetic mice experienced an impairment of flow compensation in the leptomeningeal collateral circulation, a more marked reduction of blood flow in the cortical penetrating arterioles bordering the MCA and ACA, and a delay in the adaptation of the CW; contributing to increased hemodynamic compromise and potentiating the risk of stroke or TIA.

Materials and Methods

Animals and Housing

This study was approved by the San Francisco VAMC Animal Care and Use Committee. The *db/db* mouse (B6.BKS(D)-Lepr<*db/db*>/J) carrying a mutation in the leptin receptor gene is a well-established rodent model of obesity-induced type 2 diabetes[10]. Heterozygous *db*/+ (B6.BKS(D)-Lepr<*db*/+>/J) mice were chosen as the normoglycemic controls over the wild type +/+ strain because of the closer genetic background and a nearly identical cerebrovascular anatomy of the former compared to the *db/db* mice[8]. Male *db/db* and *db/+*

mice (16–20 weeks old, Jackson Laboratories, ME) were housed 4 per cage on a 12-hour dark/light cycle with access to food and water *ad libitum*. Due to the contribution of sex hormone in vascular reactivity, the current study is focused on the male sex. All procedures and analyses were conducted by examiners blinded to experimental conditions.

Unilateral common carotid artery occlusion (CCAO)

The left carotid artery (CCA) was permanently occluded with a 6-0 suture to mimic the hypoperfusion state in the human carotid artery occlusion under isoflurane anesthesia. CCAO was chosen over the internal carotid artery occlusion (ICAO) model due to technical challenge associated with the latter if performed when the animal is on its prone position with the head fixed on a stereotaxic frame during blood flow imaging.

Blood flow imaging using Doppler optical coherent tomography (DOCT) and OCT-based microangiography (OMAG)

DOCT and OMAG imaging was conducted under isoflurane anesthesia through an intact skull at baseline, immediately or 1, 7 and 14 days after unilateral CCAO[8]. A fiber-based spectral domain OCT system using a superluminescent diode (Thorlabs Inc., Newton, NJ) as the light source was employed to image blood flow, providing a ~7μm axial resolution in the air[11]. In the sample arm, a 5X scan lens (Thorlabs Inc.) was used to achieve ~14μm lateral resolution with 270μm depth of field. The linescan camera (1024 pixel detector-array, Goodrich Inc., Princeton, NJ) was used in the spectrometer with 92 kHz line rate. To image the microvasculature, the scanning produced 400 A-lines, covering a distance of ~2 mm that formed each B-frame (in fast scanning axis). In the slow axis (C-scan), comprised of 400 steps, also covering a distance of ~2 mm. At each step, B-frames were repeated 8 times. The final data cube of a 3D scan was composed of 1024×400×3200 (z-x-y) voxels, which took <18 s to acquire with an imaging rate of 180 hertz (Hz). Following data acquisition, an eigenvalue decomposition-based clutter filtering algorithm[12] was used to generate OMAG images from the 8-repeated B-frames, producing a final volumetric vascular image of 1024×400×400 (z-x-y) voxels.

Following the OMAG scan, a Doppler OMAG (DOMAG) scanning was performed covering the same area to obtain the axial red blood cell (RBC) velocity map within the cortex[13]. In contrast to the OMAG protocol, each B-scan in the DOMAG protocol consisted of 10000 A-lines by acquiring 25 A-lines at each 400 discrete steps. In the slow scan direction (C scan), there were 600 discrete steps, i.e., 600 B scans. The data cube of each processed 3D vascular image was composed of 1024×400×600 (z-x-y) voxels, which took <100 s to acquire with 6 Hz imaging speed. Doppler processing of complex signals was applied among A-lines in each step by using 3 A-line intervals to have an axial velocity range of ±6.1 mm/s. A phase variance mask was then employed to segment meaningful Doppler flow signals from the background[13]. The blood flow in the penetrating arterioles was quantified by integrating axial velocity signals corresponding to these vessels in en face DOMAG images[11]. The total blood flow in penetrating arterioles per data was estimated by averaging 15 data points from en face DOMAG images at various depths. Due to progressively increased noise caused by scar tissue that appeared to interfere more so with the processing of penetrating arterioles than the pial arteries, we quantified the longitudinal data up to 7-d and 14-d time points for

each, respectively. Data from one *db/+* and one *db/db* mouse each were excluded due to incomplete data collection for all required time points.

Quantification of anastomosis shift

At baseline and after CCAO, the anastomosis points were marked in each baseline DOCT image where the flow direction has come to an equilibrium, shown as the green to black transition in distal ACAs. The relative distance of anastomosis shift following CCAO was measured by tracing the distance of retrograde flow in the distal MCA comparing to the anastomosis points at baseline using the Image J software with magnified images. The absolute distance was determined by calibrating the pixel value with the known tile dimension of 2 mm.

Quantification of arterial diameters in the primary collateral circulation

To assess temporal adaptation after unilateral CCAO, the diameter of the vessels forming the CW and posterior circulation was measured using Image J from the montage images with DiI labeling as described previously[8]. The vessels measured include the ICA, MCA, ACA, distal part of ACA (proximal to olfactory artery, as pOA), posterior cerebral artery (PCA), PcomA, basilar artery (BA) and vertebral artery (VA). The diameter was determined according to the line perpendicular to the main direction of flow at the truncal locations. Specifically, ICA and BA were measured at the terminal portion, while MCA and ACA at the origin before the bifurcation. The proximal olfactory artery (pOA) was measured at the largest point in diameter between the origin of ACA from the point where the olfactory artery branched out. The diameter of PCA or PcomA was determined at the largest point of each vessel near the origin of PCA at which the PcomA flow joints, while VA at the vertebrobasilar junction.

Fluoro-jade C staining

Degenerating neurons were labeled by Fluorojade C as previously described[14]. In brief, brain sections were treated with 1% sodium hydroxide/80% ethanol and 0.06% potassium permanganate, stained in 0.0001% Fluoro-Jade® C (Histo-Chem Inc., Jefferson, AR), and cover-slipped with DPX (Sigma). The staining results were visualized and imaged with a Zeiss Axioscope II epifluorescence microscope using a FITC filter.

Statistical analysis

Data were expressed as MEAN ± SEM and analyzed by one-way, two-way ANOVA or one-way RANOVA using StatView (SAS Institute, Cary, NC) with Bonferroni corrections for multiple comparisons when appropriate. *P* values less than 0.05 were considered significant.

Results

db/db mice exhibit impaired leptomeningeal collateral flow compensation following carotid occlusion

To determine whether type II diabetes is associated with impaired collateral flow compensation upon unilateral CCAO, we investigated the flow characteristics in the

leptomeningeal circulation. To increase the accuracy of comparison, distal MCA branches were categorized according to branching order, with S1 most proximal to ACA while most disal to MCA[8]. There was no significant difference in baseline flow velocity, diameter and flux in the distal MCA or ACA segments determined between the two genotypes (Figure 1). Immediately following CCAO, a minor shift of the anastomosis point towards distal MCA was detected in the *db/+* mice by DOCT averaging a distance of ~0.9 mm. This shift of anastomosis points was sustained at 24 hours and 7 days after CCAO in the *db/+* mice. In contrast, there was a significantly smaller retrograde shift of anastomosis points in the *db/db* mice at all time points investigated (Figure 1A&C) suggesting an impairment in collateral compensation in the diabetic mice. The vessel diameters of distal ACA and S1 of MCA were greater in the *db/+* mice compared to the *db/db* mice after CCAO, leading to greater flux. There was a tendency for *db/+* mice to have a greater flow velocity at S1 after CCAO compared to *db/db* mice, but the difference did not reach statistical significance. The data suggest that retrograde blood filling in the distal S1 segment of the MCA from the distal ACA via the leptomeningeal anastomoses showed greater reduction in *db/db* compared to *db/+* mice after CCAO (Figure 1).

db/db mice sustain a persistent reduction of blood flow in the penetrating arterioles following CCAO in the distal MCA and ACA territories

Since penetrating arterioles are bottlenecks in the perfusion of the neocortex from the pial vessel network to the subsurface cortical microcirculation[15], we next determined the changes of blood flow dynamics in the penetrating arteriole in response to CCAO at distal ACA and MCA segments (Figure 2A). Since there was also no significant difference in total flow or in axial velocity for the penetrating arterioles at baseline between genotypes, we expressed the flow dynamics data as percent change over baseline values. The total blood flow in penetrating arterioles increased significantly at 7 days after CCAO in the *db/+* mice, whereas it decreased immediately after CCAO and never recovered the following week in the *db/db* mice (Figure 2B). There was a significant difference in the total blood flow in the penetrating arterioles in the region of interest over one week between two genotypes of mice (RANOVA: $F_{3, 24}= 3.5$; $p<0.05$). Although the mean axial velocity of RBCs passing through penetrating arterioles in *db/+* mice was increased gradually after CCAO, there was no overall difference in flow velocity between *db/+* and *db/db* mice at all three time points (Figure 2C). Our data suggest that *db/db* mice may suffer from a greater overall reduction of blood flow into the parenchyma at the borderzone of the MCA and ACA.

Although human ICA stenosis or occlusion is often associated with borderzone infarct[16], we did not detect any apparent cell death in the forebrain, including in regions bordering the MCA and ACA in either strain of mice by Fluorojade C staining during the first week after CCAO (Figure 3), suggesting that the degree of hemodynamic ischemia resulting from unilateral CCAO is relatively mild.

The circle of Willis of *db/db* mice displays a delayed adaptation in response to CCAO

To characterize the temporal adaptation of the CW after unilateral CCAO, we examined the diameter of the major arteries labeled with DiI (Figure 4A) at baseline, 1, 7 and 14 days after CCAO. There was no significant difference found in diameter between baseline and any

given time point after CCAO of the CW arteries of the contralateral hemisphere in either genotype (Figure 4C). *db/+* mice experienced a significant but only temporary decrease in the ipsilateral PCA diameter 1d after CCAO, whereas a significant increase in the pOA and BA diameters was found on D14. The recovery of the ICA in *db/+* mice began even earlier on D7 and persisted through D14 (Figure 4BC). In contrast, *db/db* mice showed an early and significant narrowing of the ICA and PCA, and only the former had significant recovery and growth by D14. In general, the mean diameters of the ipsilateral ICA and PCA had decreased by 20% the day after CCAO in *db/db* mice, yet they were not restored to baseline size until at least one week later. This disparity in the major arterial response to unilateral CCAO resulted in significantly smaller truncal diameters in the ICA, MCA and BA on D1, and the PCA on D7 in *db/db* mice compared to *db/+* mice, pointing to an impairment in flow compensation via the CW in the diabetic mice. Except for the BA, all other major arteries in the CW of *db/db* mice had recovered in vessel size by D14 (Figure 4C). The diameter of the Pcom is very variable, indicating a large biological variance in Pcom patency or configuration among mice.

Discussion

While experimental and clinical data suggest that metabolic syndrome is associated with poor anatomical collateral status during acute ischemic stroke, it is unclear how and to what extent the collateral flow is affected temporally following chronic cerebral hypoperfusion. Upon unilateral CCAO resulting in hemodynamic impairment resembling human carotid disease, we found that the *db/db* mice not only experienced a more severe early reduction in the vessel diameters of the ipsilateral main feeding arteries in the CW including the ICA, MCA and PCA compared to *db/+* mice, but also a delayed post-CCAO adaptation by one to two weeks, suggesting that the *db/db* mice may suffer from a more severe hemodynamic compromise as a consequence. Additionally, in contrast to their normoglycemic counterparts, the *db/db* mice were less capable of equalizing the perfusion deficit in the distal MCAs by dilating the distal ACAs acutely after unilateral CCAO, leading to reduced flow in the borderzone of the distal MCAs. The deficit in flow compensation in the pial collaterals also propagated to a persistent reduction of blood flow in the penetrating arterioles in the distal MCA and ACA territories, potentiating chronic perfusion deficiency in the parenchyma. Unexpectedly, the diminished pial collateral compensation and the perfusion deficiency in the penetrating arterioles of the diabetic mice did not result in apparent cell loss in brain regions bordering the distal MCA and ACA, suggesting that the subacute effect of hypoperfusion induced by CCAO was mild. However, the long-term effect of CCAO-induced low perfusion has not been determined.

Symptomatic carotid occlusion in humans has an annual ischemic stroke risk of 5.5%–10% that is partially attributable to severely decreased vasodilatory capacity[17] or hemodynamic compromise[18] that is often accompanied by increased oxygen extraction fraction. However, among patients with symptomatic severe internal carotid artery (ICA) stenosis, the risk at 2 years of stroke or TIA is significantly reduced among those with angiographically defined collaterals compared to those without[4], proposing a role of collateralization in reducing stroke risk. Unilateral CCAO is associated with a decrease in CBF in the MCA territory in rodents, which can trigger retrograde compensation from the ACA network. Our data

suggest that the greater cerebral perfusion pressure drop in the distal MCA relative to ACA branches upon unilateral CCAO triggered an immediate shift of the stagnation points of the leptomeningeal anastomoses in the *db/+* mice, attempting to equalize perfusion pressure in the borderzone between the two vascular territories. This immediate retrograde shift of leptomeningeal anastomosis points in the *db/+* mice was likely enabled via the dilation of distal ACA branches signaled by fluid shear stress-induced nitric oxide (NO) release, leading to increased flow volume and/or velocity towards the MCA direction. Our data indicate that the inability in retrograde compensation of the distal MCA pial vessels in the *db/db* mice also resulted in a persistent reduction of blood flow in the penetrating arterioles beneath.

The mechanism led to the impaired retrograde compensation of pial vessel after brain ischemia is not entirely clear. A recent report suggests that elevation of intracranial pressure (ICP) after stroke may explain reduced flow through collateral vessels and penetrating arterioles they supply[19]. However, the impaired shift of the anastomosis points in the *db/db* mice after CCAO is unlikely due to increased ICP in the diabetic mice as it occurred almost instantaneously. Rather, it could result from altered myogenic tone and cerebrovascular reactivity[20, 21]. One potential mechanism of endothelial regulation of vascular tone is through NO since defective NO signaling in the diabetic mice was suggested by an earlier report, in which the phosphomimetic knock in of the eNOS restored vasodilation in the *db/db* mice[22]. Besides, being chronically hypertensive as in the db/db mice causes endothelial damage that may also lead to collateral impairment[23]. It is unlikely that the db/db mice suffered from a smaller cerebral perfusion deficit between distal MCAs and ACAs compared to db/+ mice, considering the greater reduction of anterograde flow to MCA compared to ACA as suggested by the significantly reduced truncal diameter at MCA compared to ACA ipsilateral to CCAO in the former. Although the diameters of the ipsilateral ACA and MCA main trunks have recovered 2 wks after CCAO to the size of baseline in the *db/db* mice and hence the amount of anterograde flow, those of the distal ACA and MCA S1 still remained smaller compared to *db/+* mice, reiterating the presence of other vascular or non-vascular factors contributing to the impaired flow in the distal ACAs and MCAs and downstream penetrating arterioles in the *db/db* mice.

Consistent with our finding, a recent mouse model of bilateral chronic carotid stenosis using a steel coil also detected an immediate reduction of cortical blood flow upon the induction of bilateral CCA stenosis by OCT microangiography, followed by a gradual recovery of flow over the next 27 days[24]. There was no significant decrease in the size of ACA or pOA ipsilateral to occlusion in either strain at one day after CCAO in our study, suggesting the existence of collateral compensation in the anterior circulation likely via cross flow from the contralateral ICA and azygous ACA (murine equivalent of Acom). The flow compensation in the posterior circulation appeared to be less efficient, as evidenced by the immediate reduction of ipsilateral PCA diameter in both strains, although PCA-MCA pial anastomose were not directly examined in this study. However, animal models of human diseases are prone to limitations. For example, the change of blood flow and vessel diameter in our study reflects rapid response to unilateral CCAO, which is the major limitation of this model of chronic hypoperfusion. Unlike the experimental models of complete or partial occlusion of the carotid artery unilaterally or bilaterally, human chronic hypoperfusion occurs over years

to decades, which may induce slow adaptation of the collateral circulation both at the level of CW and leptomeningeal collaterals. Considering the fact that both anatomic and functional configuration of the CW reflects the severity of carotid occlusion[25], another limitation of our model is the lack of genetic variance in the structure of collateral vessels, which often exists in the CW in humans. Furthermore, tandem lesions cause not only a higher risk but also leads to poor stroke outcome among patients with carotid stenosis due to increased hemodynamic impairment, which is not captured in the current mouse model of CCAO. On the other hand, being obese and hyperglycemic, the db/db mouse is a good animal model for the obese variant of type 2 diabetes and insulin resistance[10]. More importantly, the db/db strain also suffers from hypertension and elevated total cholesterol levels, bearing the hallmarks of metabolic syndrome[26, 27] that is associated with a poor collateral status in humans[7]. However, monogenic mutation in the leptin receptor, as in the db/db mice, is rare in the human population. Thus, future studies are warranted to confirm the hemodynamic changes observed in the current study with other models that cover the diversity seen in human diabetic patients.

Apart from the limitations of the animal model used for this study as described above, there also exists potential methodological or technical confounds. Similar to many animal studies of blood flow, our CCAO surgery and OCT imaging was conducted under isoflurane, a potent systemic vasodilator. Long term metabolic stress such as type 2 diabetes is known to alter adrenergic receptor function, and a recent report suggests that isoflurane anesthesia may impair cardiovascular function in the Zucker type 2 diabetic rats[28]. It is unclear whether isoflurane could exert a differential effect on hemodynamics in the db/db mice relative to db/+ mice during our study. Lastly, measurement of vessel diameter post mortem does not reflect in vivo dynamic remodeling of the vessel, nor does it provide information in flow volume and velocity.

In summary, our results indicate that immediately upon unilateral CCAO, in contrast to *db/+* mice, *db/db* mice were less able to dilate distal ACAs to equalize the perfusion deficit in the distal MCA branches, as reflected by a lesser retrograde shifting of flow direction towards the MCA territory and possibly resulting in a greater perfusion deficit in the penetrating arterioles. A number of major vessels forming the CW of *db/db* mice including the ICA and MCA also experienced delayed dilation compared to those of *db/+* mice in the weeks following CCAO. Our data suggest that type II diabetes is an additional risk factor for hemodynamic compromise during cerebral hypoperfusion, which may increase the severity and the risk of stroke or TIA.

Acknowledgments

Funding: This work was supported by NIH grant R01 NS071050 (JL), and Veterns Affairs merit award I01RX000655 and I01BX003335 (JL).

References

1. Vernieri F, Pasqualetti P, Matteis M, Passarelli F, Troisi E, Rossini PM, et al. Effect of collateral blood flow and cerebral vasomotor reactivity on the outcome of carotid artery occlusion. Stroke. 2001; 32:1552–1558. [PubMed: 11441200]

2. Norris JW, Krajewski A, Bornstein NM. The clinical role of the cerebral collateral circulation in carotid occlusion. Journal of vascular surgery. 1990; 12:113–118. [PubMed: 2116535]

3. Schomer DF, Marks MP, Steinberg GK, Johnstone IM, Boothroyd DB, Ross MR, et al. The anatomy of the posterior communicating artery as a risk factor for ischemic cerebral infarction. The New England journal of medicine. 1994; 330:1565–1570. [PubMed: 8177246]

4. Henderson RD, Eliasziw M, Fox AJ, Rothwell PM, Barnett HJ. Angiographically defined collateral circulation and risk of stroke in patients with severe carotid artery stenosis. North american symptomatic carotid endarterectomy trial (nascet) group Stroke. 2000; 31:128–132. [PubMed: 10625727]

5. Hendrikse J, Hartkamp MJ, Hillen B, Mali WP, van der Grond J. Collateral ability of the circle of willis in patients with unilateral internal carotid artery occlusion: Border zone infarcts and clinical symptoms. Stroke. 2001; 32:2768–2773. [PubMed: 11739971]

6. Guler S, Utku U, Aynaci O. Early clinical signs, lesion localization, and prognostic factors in unilateral symptomatic internal carotid artery occlusion. Journal of stroke and cerebrovascular diseases. 2014; 23:1908–1914. [PubMed: 24746551]

7. Menon BK, Smith EE, Coutts SB, Welsh DG, Faber JE, Goyal M, et al. Leptomeningeal collaterals are associated with modifiable metabolic risk factors. Annals of neurology. 2013; 74:241–248. [PubMed: 23536377]

8. Akamatsu Y, Nishijima Y, Lee CC, Yang SY, Shi L, An L, et al. Impaired leptomeningeal collateral flow contributes to the poor outcome following experimental stroke in the type 2 diabetic mice. The Journal of neuroscience. 2015; 35:3851–3864. [PubMed: 25740515]

9. Nishijima Y, Akamatsu Y, Weinstein PR, Liu J. Collaterals: Implications in cerebral ischemic diseases and therapeutic interventions. Brain research. 2015; 1623:18–29. [PubMed: 25770816]

10. King AJ. The use of animal models in diabetes research. British journal of pharmacology. 2012; 166:877–894. [PubMed: 22352879]

11. Baran U, Li Y, Wang RK. Vasodynamics of pial and penetrating arterioles in relation to arteriolo-arteriolar anastomosis after focal stroke. Neurophotonics. 2015; 2:025006. [PubMed: 26158010]

12. Yousefi S, Zhi Z, Wang RK. Eigendecomposition-based clutter filtering technique for optical micro-angiography. IEEE transactions on bio-medical engineering. 2011:58. [PubMed: 21216698]

13. Shi L, Qin J, Reif R, Wang RK. Wide velocity range doppler optical microangiography using optimized step-scanning protocol with phase variance mask. Journal of biomedical optics. 2013; 18:106015. [PubMed: 24165741]

14. Sun C, Sun H, Wu S, Lee CC, Akamatsu Y, Wang RK, et al. Conditional ablation of neuroprogenitor cells in adult mice impedes recovery of poststroke cognitive function and reduces synaptic connectivity in the perforant pathway. The Journal of neuroscience. 2013; 33:17314–17325. [PubMed: 24174664]

15. Nishimura N, Schaffer CB, Friedman B, Lyden PD, Kleinfeld D. Penetrating arterioles are a bottleneck in the perfusion of neocortex. Proceedings of the National Academy of Sciences of the United States of America. 2007; 104:365–370. [PubMed: 17190804]

16. Yamauchi H, Kudoh T, Kishibe Y, Iwasaki J, Kagawa S. Selective neuronal damage and chronic hemodynamic cerebral ischemia. Annals of neurology. 2007; 61:454–465. [PubMed: 17380523]

17. Markus H, Cullinane M. Severely impaired cerebrovascular reactivity predicts stroke and tia risk in patients with carotid artery stenosis and occlusion. Brain. 2001; 124:457–467. [PubMed: 11222446]

18. Flaherty ML, Flemming KD, McClelland R, Jorgensen NW, Brown RD Jr. Population-based study of symptomatic internal carotid artery occlusion: Incidence and long-term follow-up. Stroke. 2004; 35:e349–352. [PubMed: 15232124]

19. Beard DJ, McLeod DD, Logan CL, Murtha LA, Imtiaz MS, van Helden DF, et al. Intracranial pressure elevation reduces flow through collateral vessels and the penetrating arterioles they supply. A possible explanation for ‘collateral failure’ and infarct expansion after ischemic stroke. Journal of cerebral blood flow and metabolism. 2015; 35:861–872. [PubMed: 25669909]

20. Cipolla MJ, Porter JM, Osol G. High glucose concentrations dilate cerebral arteries and diminish myogenic tone through an endothelial mechanism. Stroke. 1997; 28:405–410. [PubMed: 9040698]

21. Sweet JG, Chan SL, Cipolla MJ. Effect of hypertension and carotid occlusion on brain parenchymal arteriole structure and reactivity. Journal of applied physiology. 2015; 119:817–823. [PubMed: 26294749]

22. Li Q, Atochin D, Kashiwagi S, Earle J, Wang A, Mandeville E, et al. Deficient enos phosphorylation is a mechanism for diabetic vascular dysfunction contributing to increased stroke size. Stroke. 2013; 44:3183–3188. [PubMed: 23988642]

23. Omura-Matsuoka E, Yagita Y, Sasaki T, Terasaki Y, Oyama N, Sugiyama Y, et al. Hypertension impairs leptomeningeal collateral growth after common carotid artery occlusion: Restoration by antihypertensive treatment. Journal of neuroscience research. 2011; 89:108–116. [PubMed: 21046561]

24. Srinivasan VJ, Yu E, Radhakrishnan H, Can A, Climov M, Leahy C, et al. Micro-heterogeneity of flow in a mouse model of chronic cerebral hypoperfusion revealed by longitudinal doppler optical coherence tomography and angiography. Journal of cerebral blood flow and metabolism. 2015; 35:1552–1560. [PubMed: 26243708]

25. Hartkamp MJ, van Der Grond J, van Everdingen KJ, Hillen B, Mali WP. Circle of willis collateral flow investigated by magnetic resonance angiography. Stroke. 1999; 30:2671–2678. [PubMed: 10582995]

26. Kennedy AJ, Ellacott KL, King VL, Hasty AH. Mouse models of the metabolic syndrome. Disease models & mechanisms. 2010; 3:156–166. [PubMed: 20212084]

27. Panchal SK, Brown L. Rodent models for metabolic syndrome research. Journal of biomedicine & biotechnology. 2011; 2011:351982. [PubMed: 21253582]

28. Bussey CT, de Leeuw AE, Lamberts RR. Increased haemodynamic adrenergic load with isoflurane anaesthesia in type 2 diabetic and obese rats in vivo. Cardiovascular diabetology. 2014; 13:161. [PubMed: 25496763]

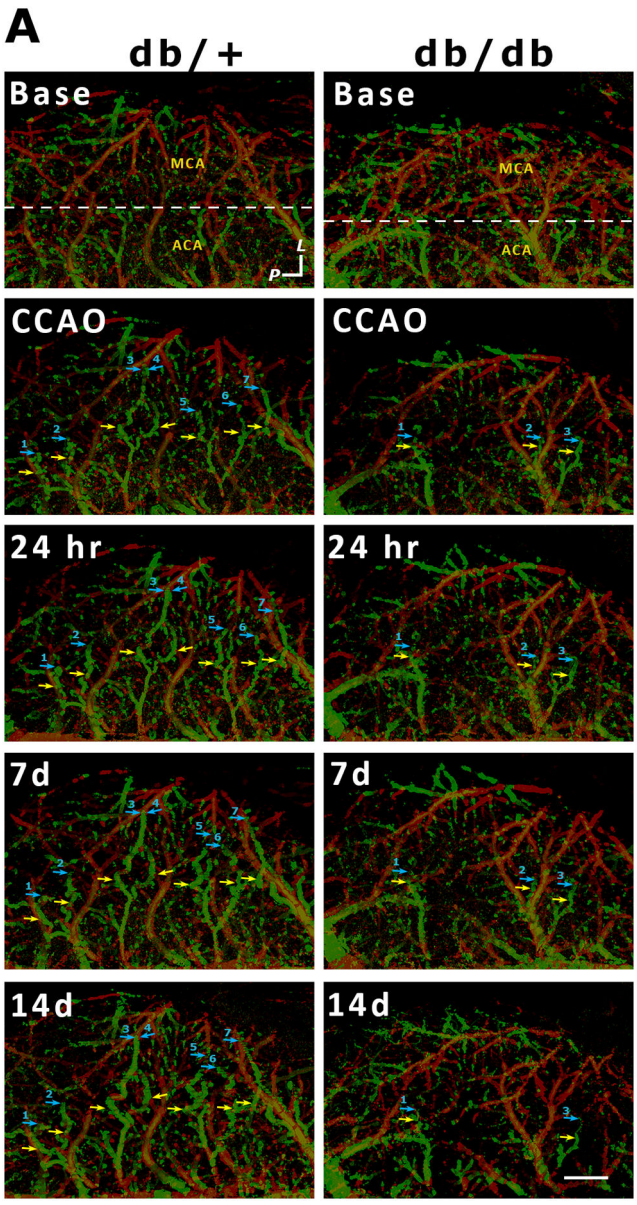

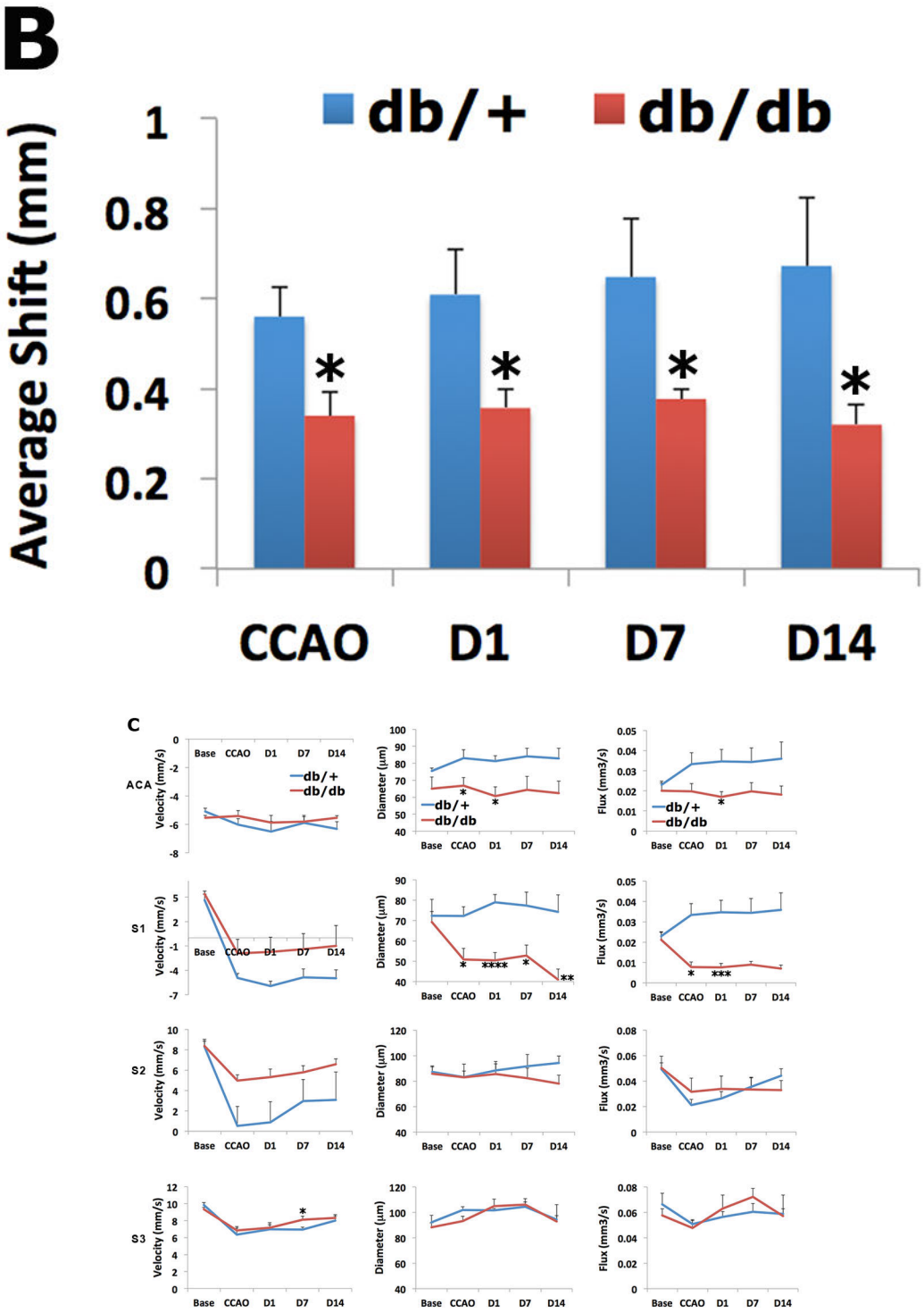

Figure 1. Chronic hypoperfusion induces retrograde shift of anastomosis points in the leptomeningeal collaterals towards multiple distal MCA branches

A, Representative DOCT images from *db/+* and *db/db* mice at baseline and various time points following unilateral (left) common carotid artery occlusion (CCAO). The anatomic orientation of the brain is indicated with arrows pointing to the lateral (*L*) and posterior (*P*)

directions. The direction of blood flow is color-coded, with the blood flowing towards the scanning probe beam coded designated as red, and the opposite direction as green. Dotted white line marks the divide between MCA and ACA territory at base line. Immediately following CCAO, a relatively mild ischemic condition compared to distal MCAO, a minor shift of the anastomosis point towards distal MCAs was detected in the normoglycemic *db/+* mice by DOCT, and sustained at all time points investigated after CCAO. Yellow and blue arrows indicated the various anastomosis points as numbered before and after the shift, respectively. Compared to *db/+* mice, *db/db* mice showed significantly reduced retrograde shift towards distal MCAs. Scale bar: 1 mm. ***B***, Measurement of the average shift of anastomoses points after CCAO compared with those at baseline in each strain. The average shift of anastomosis points towards distal MCA is significantly longer in the *db/+* compared to *db/db* mice at all time points after CCAO. ***C***, Quantification of temporal flow characteristics indicated that there was no significant difference in flow velocity, diameter or RBC flux (flux= $v\pi R^2$) between *db/+* and *db/db* mice at baseline in distal ACA and the 3 segments of distal MCA (S1, S2 and S3, with S1 most distal to MCA). After CCAO, flow velocity decreased in S1 and S2 of MCA and the direction of flow was reversed at S1 in both strains. Following CCAO, *db/+* mice showed significant higher retrograde flow velocity at S1, greater vessel diameter as well as flux at distal ACA and S1 compared to *db/db* mice. These findings suggest that the *db/db* mice had diminished leptomeningeal collateral flow compensation during chronic hypoperfusion compared to *db/+* mice. N= 5/group. **P*<0.05; ***P*<0.01; ****P*<0.005; *****P*<0.001.

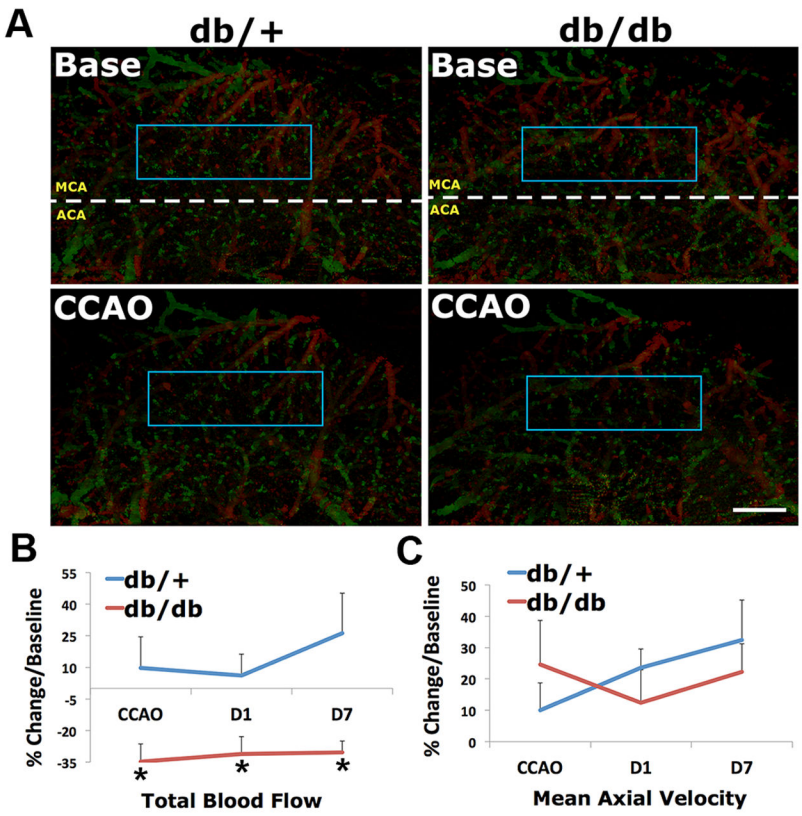

Figure 2.

Blood flow dynamics in the penetrating arterioles within the distal MCA territory. ***A***, Representative DOCT images at baseline and after CCAO similar to figure 1. The blue rectangles define the region of interest for the analysis of flow dynamics of the penetrating arterioles. Scale bar, 1 mm. ***B***, Total blood flow changes after CCAO for various time points compared to baseline. *db/db* mice had significantly reduced total blood flow in the penetrating arterioles after CCAO at the time points indicated relative to baseline. *p<0.05. C, There was no significant difference in mean axial velocity changes between *db/+* and *db/db* mice at any time point investigated. N= 5/group.

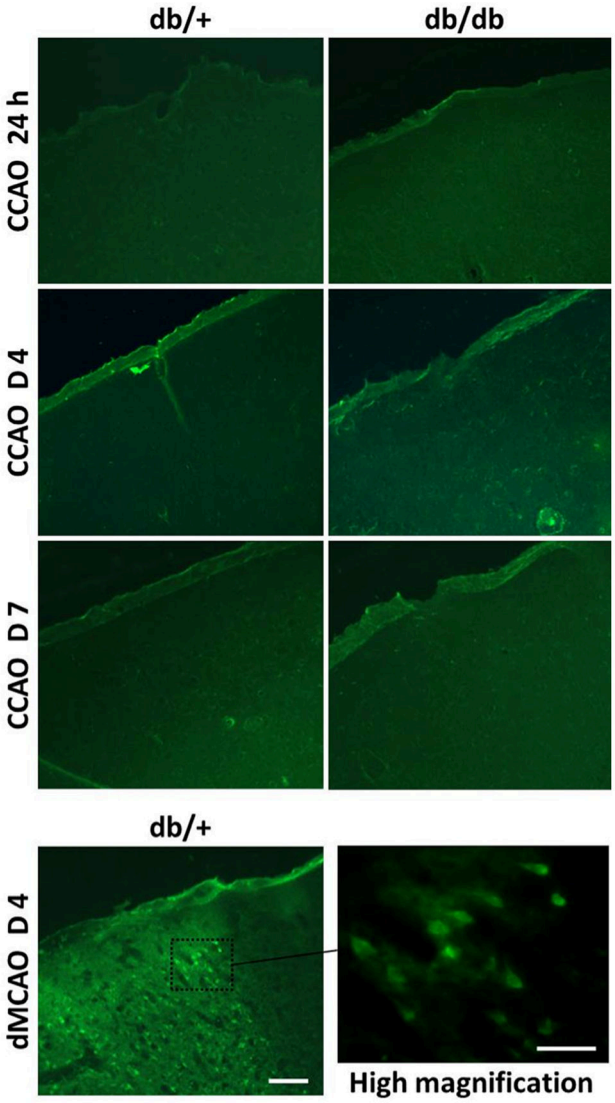

Figure 3.

Representative images of fluorojade C staining at 24 hours, 4 and 7 days after left CCAO. There was no apparent cell death at the borderzone area of left cortex in either *db/+* or *db/db* mice at any above time point, in contrast to many fluorojade C labeled degenerating neurons seen 4 days after distal MCAO. Scale bars: 100 μm (left) and 25 μm (high magnification). N=6/group.

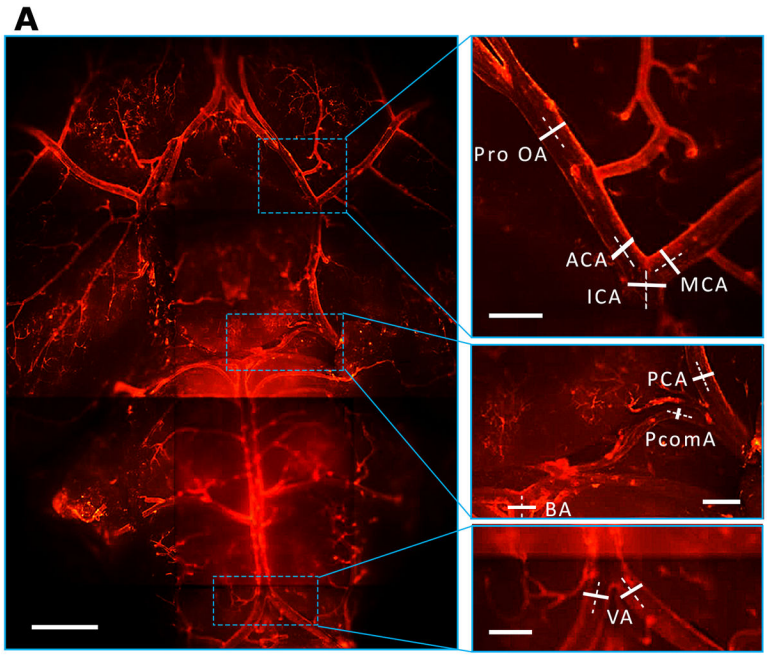

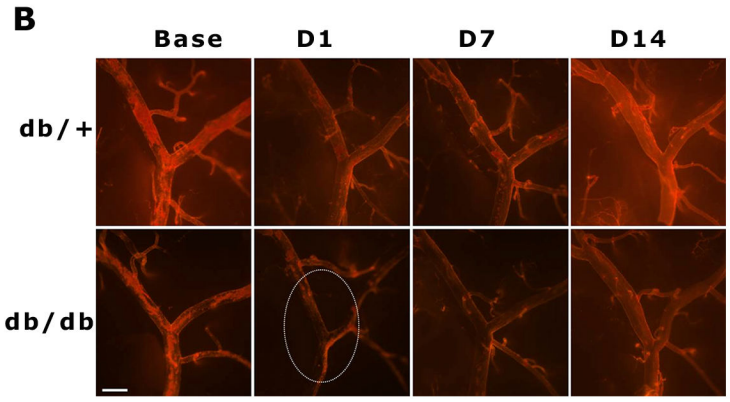

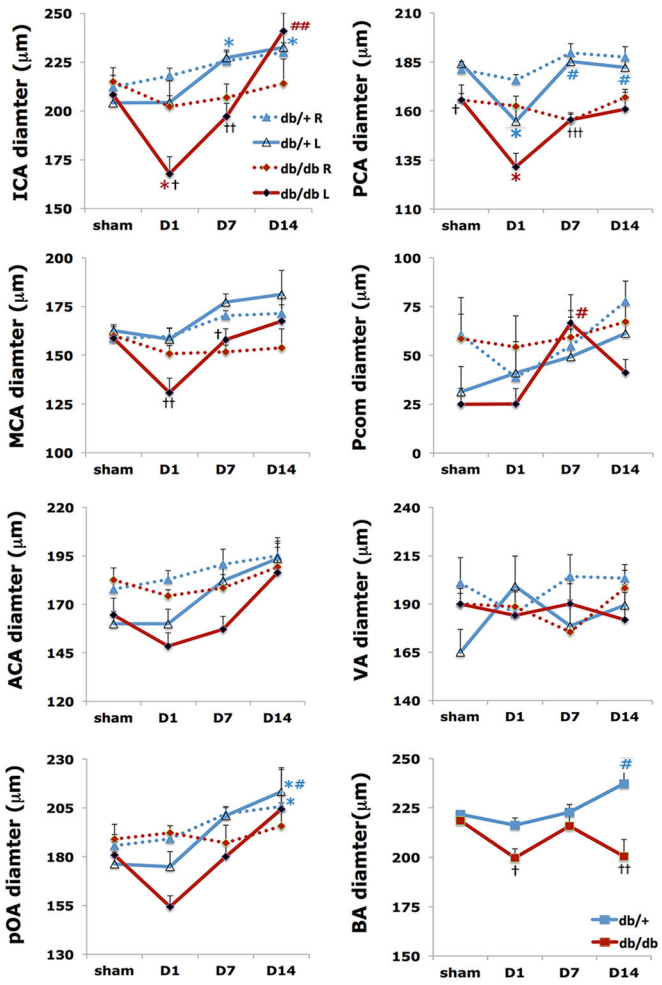

Figure 4.

The temporal adaptation of the circle of Willis (CW) after left CCAO. *db/db* mice displayed an impaired compensation of collateral flow and delayed recovery of some vessel diameters compared to *db/+* mice. ***A***, Arteriograms of the CW labeled with DiI from a sham mouse. Right column indicated the locations of diameter measurement made in each vessel in magnified views. Scale bars: 1 mm (left panel) and 250 μm (right panels). ***B***, Representative DiI images showing temporal changes of diameters in left ICA, MCA, ACA and pOA after left CCAO. The diameters of the each vessel in left anterior part of circle of Willis in *db/db* at 1 day after CCAO were significantly reduced (white dotted circle) compared to those in *db/+*, suggesting that the *db/db* mice suffered from a more severe flow reduction after left CCAO. Scale bar: 250um. ***C***, Temporal changes of the diameter of the vessels forming the CW at baseline (sham) and at various time points after CCAO. *db/db* mice showed a significant reduction of the diameter of ipsilateral ICA and PCA at 1 day after left CCAO. There were significant differences in the diameters of left ICA and left MCA at 1 and 7 days after CCAO between two strains, suggesting a delay in the growth of the primary collaterals in the diabetic mice following CCAO. Except for BA, CW collaterals of the *db/db* mice reached similar sizes as those in the *db/+* mice at 14 days after CCAO. Red and blue * were used to label significant differences between baseline and specified time points after CCAO

for the ipsilateral arteries (L) of *db/+* and *db/db*, respectively, whereas # labeled significant differences between D1 and specified time points after CCAO. Black† labeled significant differences in arterial diameters between the *db/+* and *db/db* at specified time points. **p*<0.05; †*p*<0.05; ††*p*<0.0; ††† *p*<0.001. N=5–10/group.